

RESEARCH REPORT

Coordinated control of Notch/Delta signalling and cell cycle progression drives lateral inhibition-mediated tissue patterning

Ginger L. Hunter^{1,2,*}, Zena Hadjivasiliou^{3,4}, Hope Bonin¹, Li He⁵, Norbert Perrimon⁵, Guillaume Charras^{2,6,7} and Buzz Baum^{1,2,*}

ABSTRACT

Coordinating cell differentiation with cell growth and division is crucial for the successful development, homeostasis and regeneration of multicellular tissues. Here, we use bristle patterning in the fly notum as a model system to explore the regulatory and functional coupling of cell cycle progression and cell fate decision-making. The pattern of bristles and intervening epithelial cells (ECs) becomes established through Notch-mediated lateral inhibition during G2 phase of the cell cycle, as neighbouring cells physically interact with each other via lateral contacts and/or basal protrusions. Since Notch signalling controls cell division timing downstream of Cdc25, ECs in lateral contact with a Delta-expressing cell experience higher levels of Notch signalling and divide first, followed by more distant neighbours, and lastly Delta-expressing cells. Conversely, mitotic entry and cell division makes ECs refractory to lateral inhibition signalling, fixing their fate. Using a combination of experiments and computational modelling, we show that this reciprocal relationship between Notch signalling and cell cycle progression acts like a developmental clock, providing a delimited window of time during which cells decide their fate, ensuring efficient and orderly bristle patterning.

KEY WORDS: Notch signalling, Cell cycle, Lateral inhibition, Patterning, G2 phase

INTRODUCTION

In the *Drosophila* notum, Notch-mediated lateral inhibition drives the emergence of a patterned array of microchaete, or small mechanosensory bristles, ~8–18 h after pupariation (AP) at 25°C (Fig. 1A; Movie 1) (Simpson et al., 1999; Furman and Bukharina, 2008; Cohen et al., 2010). Cells with low levels of activated Notch signalling adopt a sensory organ precursor cell (SOP) fate, and divide to give rise to the microchaete lineage (Simpson, 1990). Moreover, SOPs express high levels of neural precursor genes and Delta ligand (Muskavitch, 1994; Parks et al., 1997), which activates

Notch signalling in surrounding cells to prevent them from adopting a neural fate (Muskavitch, 1994). In this way, Notch/Delta signalling breaks symmetry to pattern the tissue (Parks et al., 1997). Notch signalling in this tissue is not limited to lateral cell contacts: a network of dynamic, actin-based protrusions at the basal side of the epithelium aids signal propagation over longer distances (de Jossineau et al., 2003; Cohen et al., 2010). This type of protrusion-mediated signalling (Hamada et al., 2014; Kornberg and Roy, 2014; Khait et al., 2016), it has been argued (Cohen et al., 2010, 2011), helps ensure the gradual emergence and refinement of a pattern of well-spaced SOPs.

Work across eukaryotic systems suggests that the decision to exit the cell cycle and divide often occurs in G1 (Vidwans and Su, 2001; Lee and Orr-Weaver, 2003). Nevertheless, some cell fate decisions, including the development of macrochaete (Usui and Kimura, 1992; Kimura et al., 1997; Nègre et al., 2003), appear to be made during passage through G2. In this paper, we show how feedback between cell fate-determining signals and progression through mitosis coordinates timely epithelial patterning in the fly notum.

RESULTS AND DISCUSSION

During notum development, all ECs divide once (Bosveld et al., 2012) (Movie 1), before undergoing terminal differentiation. At the same time, an initially disordered array of cells expressing proneural genes is refined to generate an ordered pattern of bristles in adults (Cohen et al., 2010; Protonotarios et al., 2014) (Fig. 1A). By simultaneously following cell division and patterning in this tissue, we find that local patterns of division timing correlate with proximity to SOPs (Fig. 1B–D). ECs sharing long cell-cell interfaces with SOPs, hereafter termed primary neighbours (1N), divide first. These are followed by next-nearest ECs, or secondary neighbours (2N), which contact SOPs via dynamic basal protrusions alone (Cohen et al., 2010). SOPs divide last (Fig. 1C). The local spatiotemporal pattern of divisions is robust, as indicated by a ratio of division times for neighbours surrounding each SOP of <1 (Fig. 1E), even though the timing of bristle-row patterning is developmentally staggered (Usui and Kimura, 1993; Parks et al., 1997). Moreover, ECs that transiently express proneural markers (Cohen et al., 2010) (Fig. S1A–C), including Delta (Kunisch et al., 1994), before assuming an EC fate accelerate G2 exit in their EC neighbours (Fig. 1F).

The local pattern of EC division is Notch dependent

If lateral inhibition cues division timing, as suggested by these observations, we can make the following predictions. First, for each SOP neighbourhood, there should be differences in the intensity of Notch signalling between primary and secondary neighbours. Second, perturbing Notch signalling should disrupt the pattern of cell divisions. To test this, we visualized signalling dynamics using *Notch-nls::sfGFP* (N^{sfGFP}) (Fig. 2A,B). N^{sfGFP} is a nuclear localized, PEST-tagged (unstable), super-folder GFP expressed

¹MRC-Laboratory for Molecular and Cell Biology, University College London, London WC1E 6BT, UK. ²Institute of Physics of Living Systems, University College London, London WC1E 6BT, UK. ³Centre for Mathematics, Physics, and Engineering in the Life Sciences and Experimental Biology, University College London, London WC1E 6BT, UK. ⁴Department of Genetics, Evolution and Environment, University College London, London WC1E 6BT, UK. ⁵Howard Hughes Medical Institute, Department of Genetics, Harvard Medical School, Boston, MA 02115, USA. ⁶London Centre for Nanotechnology, University College London, London WC1E 6BT, UK. ⁷Department of Cell and Developmental Biology, University College London, London WC1E 6BT, UK.

*Authors for correspondence (g.hunter@ucl.ac.uk; b.baum@ucl.ac.uk)

 G.L.H., 0000-0001-7022-9482

This is an Open Access article distributed under the terms of the Creative Commons Attribution License (<http://creativecommons.org/licenses/by/3.0>), which permits unrestricted use, distribution and reproduction in any medium provided that the original work is properly attributed.

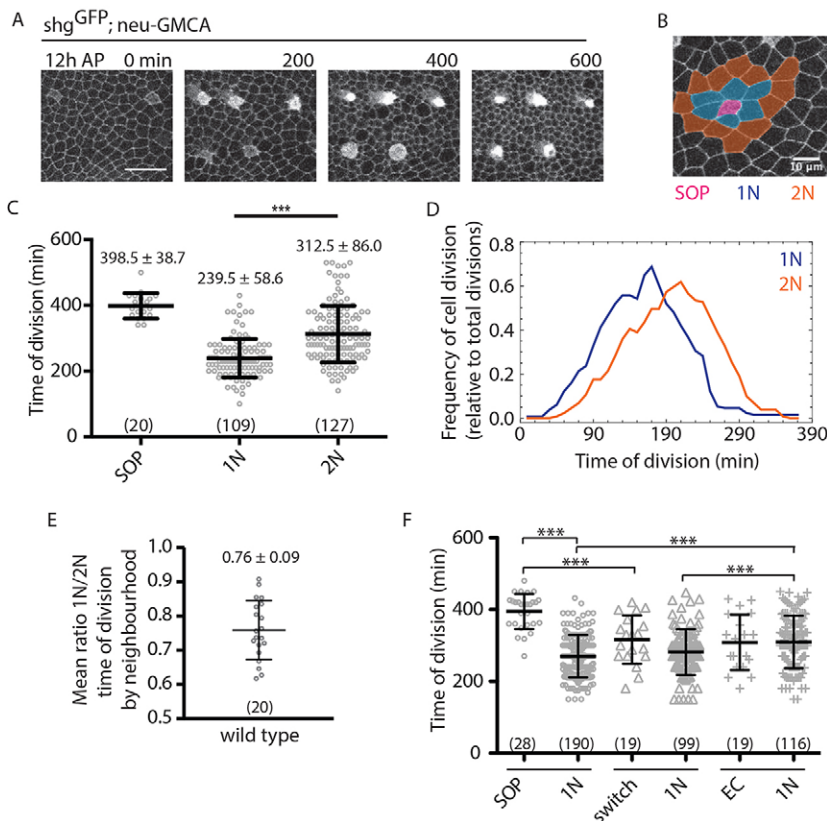


Fig. 1. Spatiotemporal patterning of notum cell divisions. (A) Pupal notum expressing *Shotgun^{GFP}* (cell boundaries), and *nGMCA* (SOPs) over time. Posterior to the left, anterior to the right. Scale bar: 25 μ m. (B) SOP 'neighbourhood': SOP (pink) with primary (1N; blue) and secondary (2N; orange) neighbours. Scale bar: 10 μ m. (C) Time of cell division for the genotype shown in A; *N*=2 pupae. (D) Line graph of the data shown in C. (E) Mean ratio of local SOP neighbourhood division timing, genotype as in A. *N*=2 nota; *n*=20 SOPs, 109 1Ns, 127 2Ns. (F) Division timing of SOPs, 'switch' cells (*neu-GMCA*-expressing cells that switch to EC fate) and ECs and their respective 1Ns in *shotgun^{GFP}; neu-GMCA* pupae (*N*=3). ****P*<0.001 (unpaired two-tailed *t*-test for pairs indicated). Mean \pm s.d. shown. (n)=number of cells.

downstream of a minimal GBE-Su(H) promoter (L.H. and N.P., unpublished) (Li et al., 1998; Furriols and Bray, 2001) (Fig. S1A–C).

At 12 h AP, *N^{sfGFP}* is visible in EC rows in which bristle formation occurs (Fig. S1A) (Usui and Kimura, 1993). Notch signalling increases nearly linearly in ECs until division (Fig. 2C; Fig. S1D–G). The rate of response, which functions as a measure of signal strength, is higher in primary than secondary neighbours (Fig. 2C,D). The peak *N^{sfGFP}* signal is similar for both neighbours when measured across the tissue (Fig. 2E). However, the local ratio of *N^{sfGFP}* signal prior to division is >1 (Fig. 2F), suggesting that primary ECs receive a higher Delta signal from individual SOPs than do secondary ECs.

To test whether *N^{sfGFP}* signal and division timing in ECs depends on Delta expression in SOPs, we measured local *N^{sfGFP}* signal following laser ablation of SOPs (Fig. S1H). Under these conditions, *N^{sfGFP}* signal accumulation halts in primary and secondary ECs, but continues to increase in ECs proximal to both the wound and intact SOPs (Fig. S1I), as expected if the signal depends on a Delta input from the ablated SOP. Relative to controls, EC divisions are delayed following local SOP loss (Fig. S1J). Additionally, we found that dominant-negative Delta ligand (*Delta^{DN}*) overexpression in SOPs decreases *N^{sfGFP}* signal in neighbouring ECs (Fig. 2G,H) (Herranz et al., 2006). Together with the ablation data, this shows that *N^{sfGFP}* signal in ECs is dependent upon Delta-expressing SOPs.

Next, we examined the effects of disrupting Notch signalling on cell division timing by overexpressing *Delta^{DN}* in SOPs (Fig. 2I) or using RNAi against Suppressor of Hairless [*Su(H)*], an essential component of Notch-targeted gene expression (Lehman et al., 1999; Furriols and Bray, 2001) across the tissue. *Delta^{DN}* expression did not disrupt the pattern of local division timings but was sufficient to

delay division of neighbouring ECs, as expected if Delta signal promotes division. *Su(H)* depletion blocks divisions within the *pnr* domain in the majority of animals (*N*=4/6 pupae), and later leads to tissue failure. In the remaining animals (*N*=2/6 pupae), which may express levels of *Su(H)* activity sufficient for tissue survival, divisions are delayed and the local pattern of divisions is perturbed in regions where microchaete are formed (Fig. 2J). Therefore, local cell division timing is dependent on Notch-mediated lateral inhibition.

The local timing of EC division is dependent on Cdc25 and Wee1

At the onset of bristle patterning, cells in the notum are arrested in G2 of the cell cycle. All cells express a nuclear Fucci-GFP marker (Fig. S2A) but do not stain for 5-ethynyl-2'-deoxyuridine (EdU), a marker for ongoing DNA replication (Fig. S2B). In many systems, G2 exit is regulated by the phosphatase *Cdc25*, encoded by *Drosophila string* (*stg*) (Edgar and O'Farrell, 1989; Courtot et al., 1992), which catalyses removal of an inhibitory phosphate group (added by the kinases *Wee1* and *Myt1*; Price et al., 2000; Jin et al., 2008) from a regulatory tyrosine on Cdk1. *Wee1* and *Myt1* function in opposition to *Cdc25* in many systems (Vidwans and Su, 2001), sometimes redundantly (Jin et al., 2008).

To test whether *Cdc25* and the kinases *Wee1* and *Myt1* regulate G2 exit in the notum, we expressed dsRNAs targeting these regulators under *pnr-GAL4*. *stg* RNAi expression delays EC division timing, prevents patterned divisions, and in some cases blocks division altogether (Fig. 3A,A'; Fig. S2C). Conversely, *wee1*- or *myt1* RNAi expression throughout the notum causes precocious EC entry into mitosis (Fig. 3B,C). Loss of *stg*, *wee1* or *myt1* expression does not affect the timing of the first division of SOPs (Fig. 3A–C) (which are subject to additional regulation; Ayeni et al., 2016).

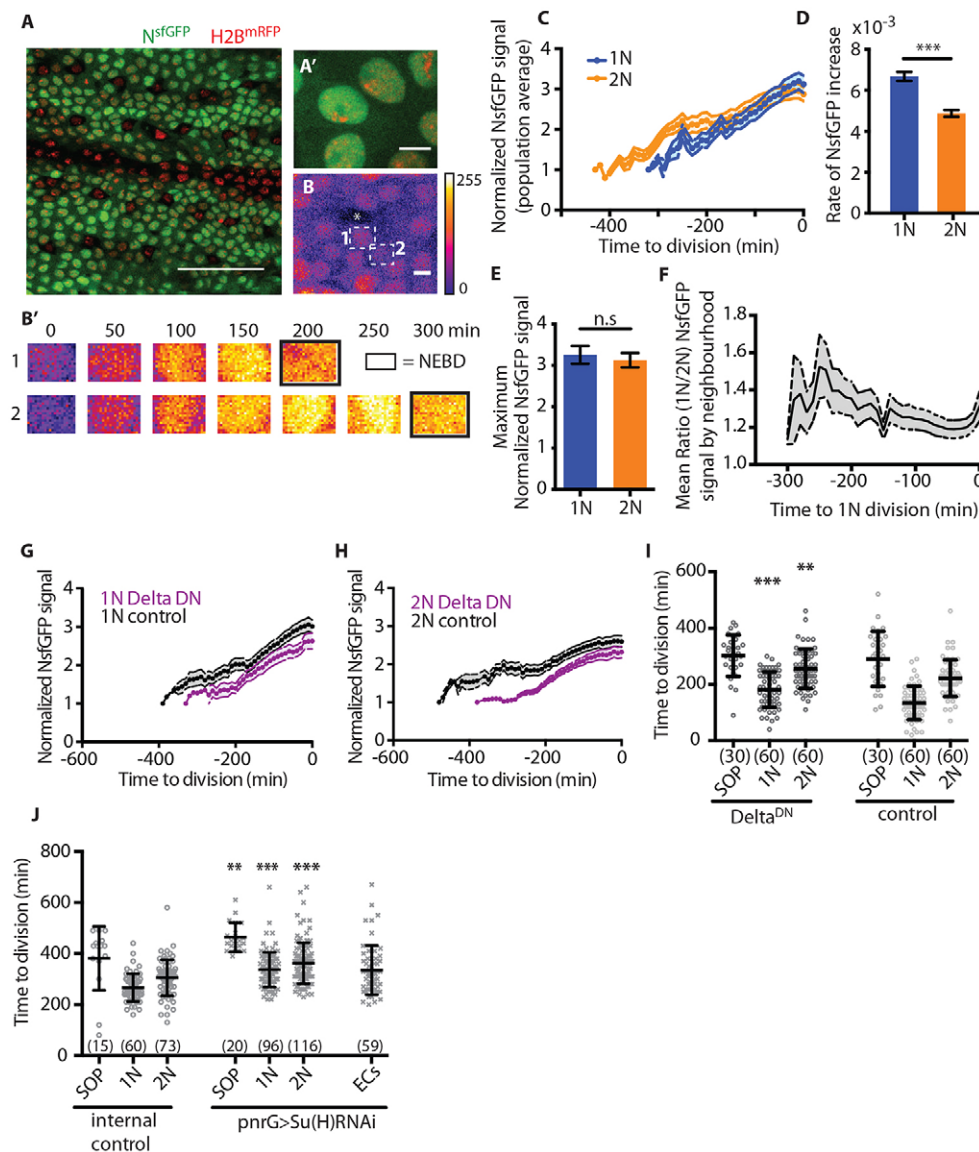


Fig. 2. Cell division timing depends on Notch signalling. (A) NsfGFP expression pattern at 12 h AP. H2BmRFP labels nuclei. Scale bar: 50 μ m. (A') Higher magnification image of A. Scale bar: 5 μ m. (B) False-coloured panel of NsfGFP-expressing ECs. Asterisk indicates SOP. Primary (1) and secondary (2) neighbours are indicated by dashed boxes. Scale bar: 5 μ m. (B') Time series of nuclear ROIs for cells 1 and 2 until nuclear envelope breakdown (NEBD; indicated by black boxes), leading to transient depletion of signal. (C) NsfGFP dynamics in ECs ($n=29$ each, $N=3$). (D) Rate of NsfGFP increase for the data shown in C. (E) Maximum normalized NsfGFP signal for the data shown in C. (F) Mean ratio of local SOP neighbourhood NsfGFP signal ($n=27$ SOP, 133 each EC type; $N=3$). (G–I) neur-GAL4 expression of Delta^{DN} reduces Notch signalling in wild-type 1N (G) or 2N (H) cells ($n=16$, $N=2$) versus control (UAS-lifeActRuby, $n=30$, $N=3$) and delays cell division timing in Shotgun^{GFP}; neu-GAL4, UAS-GMCA>UAS-Delta^{DN} pupae (I) ($N=3$). (J) Cell division timing in Shotgun^{GFP}; pnrGAL4>UAS-Su(H) RNAi pupae relative to control ($N=2$). ECs, epithelial cells in regions lacking differentiating SOPs. Mean \pm s.e.m. for C, F, G, H; mean \pm s.d. for D, E, I, J. n.s., not significant; ** $P<0.01$; *** $P<0.0001$ by unpaired, two-tailed, t -test as indicated compared with control of the same type (i.e. RNAi-1N to control-1N). (n)=number of cells.

Together, these results support a model in which the opposing activities of Cdc25 and Wee1/Myt1 regulate EC division timing.

Conversely, the duration of G2 might influence Notch signalling. Because NsfGFP decreases immediately after EC divisions, but prior to SOP division (Fig. 3D,E), we investigated whether division renders ECs refractory to Delta signal. To test this, we quantified NsfGFP dynamics in cells in which the length of G2 was altered by *stg* RNAi or *wee1* RNAi. As expected if division curtails signalling, NsfGFP expression was retained in cells with extended G2 (Fig. 3D–F), but was lost in those that divided prematurely (Fig. 3D,E). The timing of G2 exit appears to be crucial for a robust Notch response in ECs, which is terminated following division.

Relative timing of SOP cell and EC division is crucial for bristle patterning

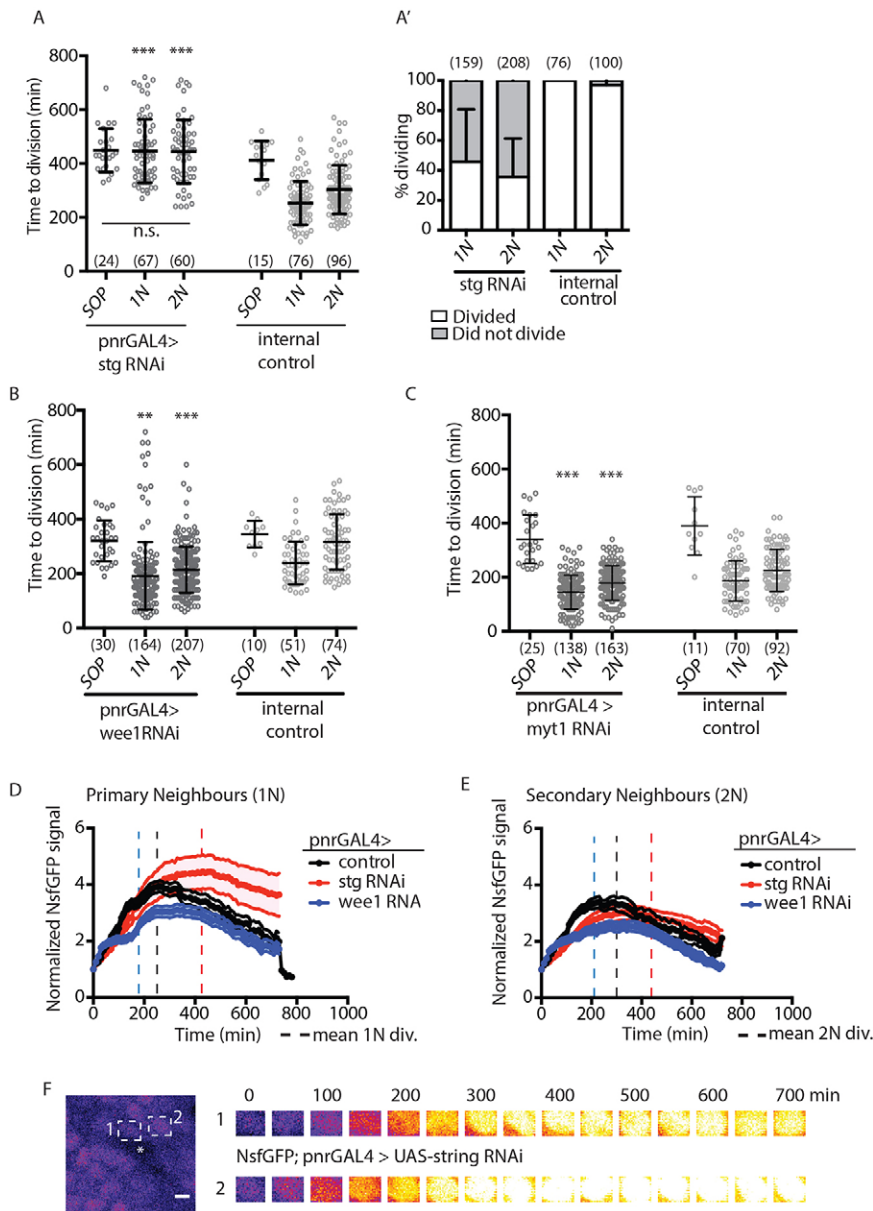
To examine the consequences of the observed coupling between Notch signalling and cell cycle progression on tissue patterning, we developed a mathematical model of lateral inhibition (see supplementary Materials and Methods for details) (Cohen et al., 2010; Sprinzak et al., 2010). The model follows the dynamics of transmembrane Notch receptor (N), Delta ligand (D) and

intracellular Notch (R ; i.e. activated Notch) in a 2D array of cells. We model basal protrusion-mediated signalling (relevant for 1N, 2N) and signalling mediated by apicolateral cell-cell contacts (relevant for 1N only). The level of apical and basal signalling is weighted by α_a and α_b , respectively; we set $\alpha_a > \alpha_b$ following previous observations (Benhra et al., 2010; Cohen et al., 2010). To couple signalling and division, we allow cells to divide with a probability p_d at any time step, as a function of R , so that:

$$p_d = \frac{R^q}{K_R^q + R^q}.$$

The value of K_R determines the window of Notch response for which division becomes likely (Fig. S3A). To mimic events in the tissue, after division the developmental fate of a cell is locked and it no longer participates in lateral inhibition.

To model a wild-type tissue in which Notch signalling drives EC division, we set $q=5$ and $K_R=200$ (Fig. 4A; Fig. S3B–D). Under these conditions, primary neighbours divide first, followed by secondary neighbours (Fig. 4B,C), consistent with spatiotemporal patterning of EC division *in vivo* (Fig. 1C–E); this delay persists



even when $\alpha_a = \alpha_b$ (i.e. amount of apical or basal Delta is equivalent; Fig. S3E). The overall profile of Notch expression at division in neighbours generated by the model (Fig. S3D) is comparable to that seen *in vivo* (Fig. S1D–G). At the tissue level, the time taken to reach a stable pattern increases with K_R (Fig. S3F), suggesting that for a given developmental time window, there is an optimal range of Notch response for determining cell fate.

Using this model, we tested the effect of uncoupling EC division timing from Notch signalling: any (non-Delta) cell may divide with a fixed probability p_d , that is independent of Notch. This leads to sparse patterns with few Delta cells, particularly for large values of p_d (Fig. 4D; Fig. S3G). We also tested the effect of primary and secondary neighbours dividing at the same time (Fig. S3H) by only allowing uniform protrusion-based signalling – where signal strength is independent of protrusion length. Under these conditions the pattern is again ordered but sparse. Together, this suggests that the delay in division in cells with low Notch expression is important for patterning. Because patterning is not uniform across the notum, this delay (Fig. 1C; Fig. 4B,C) preserves

a pool of ECs that, because they lie far from SOPs and receive a weak Delta-input signal (Fig. 2D–F), have the potential to switch fate to help refine the bristle pattern as it emerges (Movie 1).

Next, we investigated the impact of changing the relative timing of SOP and EC divisions. When we couple Delta expression to a fixed value of p_d , so that cells for which Delta expression exceeds a threshold (D_{th}) can divide, clusters of Delta-expressing cells form that disrupt the pattern (Fig. 4E). This is because, under the model, a Delta cell that divides no longer inhibits its neighbours from acquiring an SOP fate. To test whether we observe similar behaviour *in vivo*, we overexpressed String in SOPs (Fig. 4F–I). This disrupts tissue patterning in two ways. First, we observe cells expressing low levels of neuralized reporter dividing early. Frequently, one daughter cell develops into an SOP, and the other is inhibited from doing so, switching to EC cell fate (47.5%, $n=61$; $N=3$) or delaminating (9.8%). In other cases, both daughter cells form SOPs (26.2%; Fig. 4H) and paired bristles (Fig. S3I). Second, we observed secondary neighbours of early dividing SOPs adopting an SOP fate (Fig. 4I), as in the model, probably following the loss of

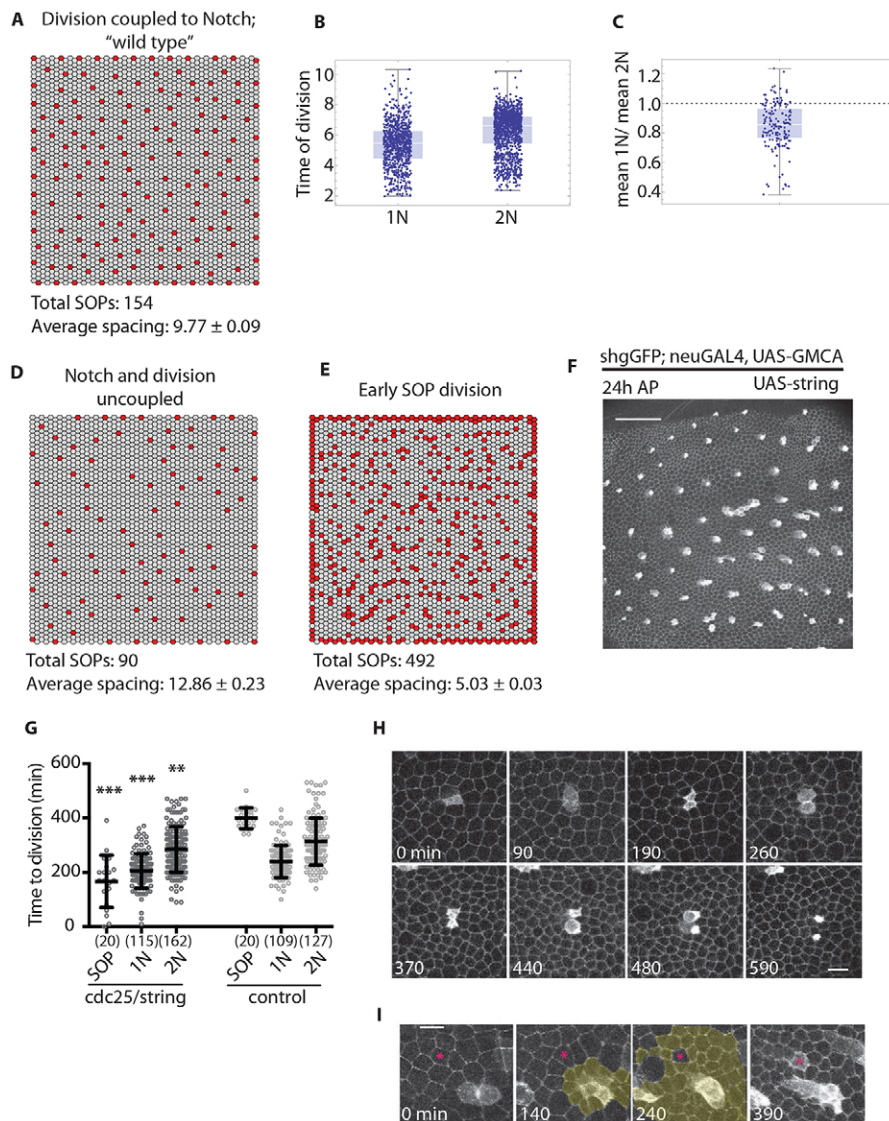


Fig. 4. Cell division timing is crucial for SOP patterning. (A) Model output for 'wild type' simulation ($K_R=200$, $q=5$). Average spacing is the mean \pm s.e.m. distance between each SOP (red) and its ten nearest SOPs. (B) Simulation results for cell division timing in 1N and 2N for the wild-type model described in A. (C) Ratio of mean time of division for 1N and 2N in the model. (D) Model output when Notch signalling and division timing are uncoupled, $p_d=0.005$ (any non-Delta cell [$D<1$] divides with probability p_d). (E) Model output when SOPs are forced to divide early (Delta cells [$D>1$] divide with probability $p_d=0.0001$). Red, Delta expressing SOPs ($D>1$); grey, Notch-expressing ECs. (F) Final SOP pattern in tissues with precocious SOP division. Scale bar: 50 μ m. (G) Cell division timing in Shotgun^{GFP}; neu-GAL4, UAS-GMCA>UAS-string pupae ($N=3$, mean \pm s.d.). Control: Shotgun^{GFP}; neu-GAL4, UAS-GMCA ($N=3$). (H,I) SOP 'twins' and secondary neighbour cell switching (asterisks in I), as a consequence of the precocious SOP division shown in F. Yellow, divided cells. Scale bars: 10 μ m. $**P\leq 0.01$, $***P\leq 0.001$, unpaired, two-tailed, t -test to control of same type. (n)=number of cells.

protrusion-mediated Delta signalling at division. We note that this phenotype is also observed on occasion in wild-type tissue, and is consistent with the observation that precocious SOP division terminates Delta signalling, leading to reduced levels of N^{sGFP} signal in surrounding ECs (Fig. S3J,K). These data further support our hypothesis that cell division signals the termination of lateral inhibition between SOPs and ECs.

Conclusions

The results of our experimental analysis show that Notch signalling drives EC division in the notum, coupling patterning to cell cycle progression. As shown in simulations, this aids timely and orderly patterning by taking cells 'out of the game', so that the fate of ECs is sealed before SOPs divide. The effects of re-wiring the system can be seen by the induction of premature SOP divisions, which in both experiment and model leads to the formation of excess SOPs as the result of secondary ECs changing their fate. The delay in the division of secondary and tertiary ECs, which receive a relatively weaker Delta input from local SOPs, provides a population of cells with an indeterminate fate that can be used to fill in any gaps in the pattern as it emerges. This is key to pattern refinement. Through an extended G2 phase, the system has a delimited window of time during which Notch and Delta can pattern the tissue through lateral

inhibition, before signal-induced entry into mitosis fixes the pattern, driving the process to completion.

MATERIALS AND METHODS

Fly strains

'Wild type' refers to control animals. See supplementary Materials and Methods for a full list of fly strains used.

Microscopy

White pre-pupae were picked and aged to 12 h AP at 18°C. Live pupae were dissected as previously described (Zitserman and Roegiers, 2011). Live pupae were imaged on a Leica SPE confocal, 40 \times oil immersion objective (1.15 NA) at room temperature. Fixed nota were imaged on a Leica SPE3 confocal, 63 \times oil immersion objective (1.3 NA). Datasets were captured using Leica LSM AF software.

Laser ablation

Ablations were performed with 730-nm multiphoton excitation from a Chameleon-XR Ti-Sapphire laser on a Zeiss Axioskop2/LSM510 (AIM, Zeiss). Post-ablation images were acquired as described above.

Immunofluorescence

Nota of staged pupae fixed as previously described (Zitserman and Roegiers, 2011) (see supplementary Materials and Methods for further

details). Primary antibodies were anti-GFP (1:1000; Abcam) and anti-Dlg (1:500; Developmental Studies Hybridoma Bank). Secondary antibodies were Alexa Fluor 488-conjugated anti-chicken and Alexa Fluor 568-conjugated anti-mouse (both 1:1000; Thermo Fisher Scientific). EdU staining was performed using the Click-iT EdU Imaging Kit (Thermo Fisher Scientific).

Quantification

N^{sfGFP} signal was quantified as follows: unprocessed imaging data was imported into Fiji (ImageJ, NIH). Mean pixel value for a nuclear region of interest (ROI) was taken for each time point. Normalized N^{sfGFP} is relative to N^{sfGFP} signal at t_0 . For neighbourhood measurements, nuclear ROIs were taken and averaged for four or five primary and four or five secondary ECs per SOP in bristle row 2. Internal control measurements were made in the same animals, but outside the pnr domain. For cell division timing panels, $t=0$ min at ~12 h AP. Resulting data were analysed using Prism (Graphpad) and using statistical tests as outlined in figure legends.

Mathematical model

See supplementary Materials and Methods for a full description of the mathematical model.

Acknowledgements

Laser ablation experiments were performed with the help of Jonathan Gale (UCL). We thank Jonathan Clarke (KCL) for critical reading of this manuscript. Stocks obtained from the Bloomington *Drosophila* Stock Center (NIH P40OD018537) were used in this study.

Competing interests

The authors declare no competing or financial interests.

Author contributions

G.L.H., Z.H., and B.B. wrote the manuscript. G.L.H. and B.B. designed experiments. G.L.H. performed and analysed fly experiments, aided by H.B. Z.H. designed and implemented 2D modelling. L.H. and N.P. designed, generated, and provided N^{sfGFP} fly lines. G.C. and B.B. acquired funding.

Funding

This work was supported by the National Institutes of Health [R21 to N.P.]; the Howard Hughes Medical Institute (N.P.); an Engineering and Physical Sciences Research Council Research Fellowship [EP/L504889/1 to Z.H.]; the Biotechnology and Biological Sciences Research Council [BB/J008532/1 to G.L.H.]; a Cancer Research UK fellowship (B.B.); and University College London (B.B.). Deposited in PMC for immediate release.

Supplementary information

Supplementary information available online at <http://dev.biologists.org/lookup/doi/10.1242/dev.134213.supplemental>

References

- Ayeni, J. O., Audibert, A., Fichelson, P., Srayko, M., Gho, M. and Campbell, S. D. (2016). G2 phase arrest prevents bristle progenitor self-renewal and synchronizes cell division with cell fate differentiation. *Development* **143**, 1160-1169.
- Benhra, N., Vignaux, F. O., Dussert, A., Schweisguth, F. and Le Borgne, R. (2010). Neutralized promotes basal to apical transcytosis of delta in epithelial cells. *Mol. Biol. Cell* **21**, 2078-2086.
- Bosveld, F., Bonnet, I., Guirao, B., Tlili, S., Wang, Z., Petitalot, A., Marchand, R., Bardet, P.-L., Marcq, P., Graner, F. et al. (2012). Mechanical control of morphogenesis by Fat/Dachsous/Four-jointed planar cell polarity pathway. *Science* **336**, 724-727.
- Cohen, M., Georgiou, M., Stevenson, N. L., Miodownik, M. and Baum, B. (2010). Dynamic filopodia transmit intermittent Delta-Notch signaling to drive pattern refinement during lateral inhibition. *Dev. Cell* **19**, 78-89.
- Cohen, M., Baum, B. and Miodownik, M. (2011). The importance of structured noise in the generation of self-organizing tissue patterns through contact-mediated cell-cell signalling. *J. R. Soc. Interface* **8**, 787-798.
- Courtot, C., Fankhauser, C., Simanis, V. and Lehner, C. F. (1992). The *Drosophila* cdc25 homolog twine is required for meiosis. *Development* **116**, 405-416.
- de Jossineau, C., Soulé, J., Martin, M., Anguille, C., Montcourrier, P. and Alexandre, D. (2003). Delta-promoted filopodia mediate long-range lateral inhibition in *Drosophila*. *Nature* **426**, 555-559.
- Edgar, B. A. and O'Farrell, P. H. (1989). Genetic control of cell division patterns in the *Drosophila* embryo. *Cell* **57**, 177-187.
- Furman, D. P. and Bukharina, T. A. (2008). How *Drosophila melanogaster* Forms its Mechanoreceptors. *Curr. Genomics* **9**, 312-323.
- Furriols, M. and Bray, S. (2001). A model Notch response element detects Suppressor of Hairless-dependent molecular switch. *Curr. Biol.* **11**, 60-64.
- Hamada, H., Watanabe, M., Lau, H. E., Nishida, T., Hasegawa, T., Parichy, D. M. and Kondo, S. (2014). Involvement of Delta/Notch signaling in zebrafish adult pigment stripe patterning. *Development* **141**, 318-324.
- Herranz, H., Stamatakis, E., Feiguin, F. and Milán, M. (2006). Self-refinement of Notch activity through the transmembrane protein Crumbs: modulation of gamma-secretase activity. *EMBO Rep.* **7**, 297-302.
- Jin, Z., Homola, E., Tiong, S. and Campbell, S. D. (2008). *Drosophila* myt1 is the major cdk1 inhibitory kinase for wing imaginal disc development. *Genetics* **180**, 2123-2133.
- Khait, I., Orsher, Y., Golan, O., Binshtok, U., Gordon-Bar, N., Amir-Zilberstein, L. and Sprinzak, D. (2016). Quantitative analysis of delta-like 1 membrane dynamics elucidates the role of contact geometry on notch signaling. *Cell Rep.* **14**, 225-233.
- Kimura, K., Usui-Ishihara, A. and Usui, K. (1997). G2 arrest of cell cycle ensures a determination process of sensory mother cell formation in *Drosophila*. *Dev. Genes Evol.* **207**, 199-202.
- Kornberg, T. B. and Roy, S. (2014). Cytonemes as specialized signaling filopodia. *Development* **141**, 729-736.
- Kunisch, M., Haenlin, M. and Campos-Ortega, J. A. (1994). Lateral inhibition mediated by the *Drosophila* neurogenic gene delta is enhanced by proneural proteins. *Proc. Natl. Acad. Sci. USA* **91**, 10139-10143.
- Lee, L. A. and Orr-Weaver, T. L. (2003). Regulation of cell cycles in *Drosophila* development: intrinsic and extrinsic cues. *Annu. Rev. Genet.* **37**, 545-578.
- Lehman, D. A., Patterson, B., Johnston, L. A., Balzer, T., Britton, J. S., Saint, R. and Edgar, B. A. (1999). Cis-regulatory elements of the mitotic regulator, string/Cdc25. *Development* **126**, 1793-1803.
- Li, X., Zhao, X., Fang, Y., Jiang, X., Duong, T., Fan, C., Huang, C.-C. and Kain, S. R. (1998). Generation of destabilized green fluorescent protein as a transcription reporter. *J. Biol. Chem.* **273**, 34970-34975.
- Muskavitch, M. A. T. (1994). Delta-notch signaling and *Drosophila* cell fate choice. *Dev. Biol.* **166**, 415-430.
- Nègre, N., Ghysen, A. and Martinez, A.-M. (2003). Mitotic G2-arrest is required for neural cell fate determination in *Drosophila*. *Mech. Dev.* **120**, 253-265.
- Parks, A. L., Huppert, S. S. and Muskavitch, M. A. T. (1997). The dynamics of neurogenic signalling underlying bristle development in *Drosophila melanogaster*. *Mech. Dev.* **63**, 61-74.
- Price, D., Rabinovitch, S., O'Farrell, P. H. and Campbell, S. D. (2000). *Drosophila* wee1 has an essential role in the nuclear divisions of early embryogenesis. *Genetics* **155**, 159-166.
- Protonotarios, E. D., Baum, B., Johnston, A., Hunter, G. L. and Griffin, L. D. (2014). An absolute interval scale of order for point patterns. *J. R. Soc. Interface* **11**, 20140342.
- Simpson, P. (1990). Lateral inhibition and the development of the sensory bristles of the adult peripheral nervous system of *Drosophila*. *Development* **109**, 509-519.
- Simpson, P., Woehl, R. and Usui, K. (1999). The development and evolution of bristle patterns in Diptera. *Development* **126**, 1349-1364.
- Sprinzak, D., Lakhanpal, A., LeBon, L., Santat, L. A., Fontes, M. E., Anderson, G. A., Garcia-Ojalvo, J. and Elowitz, M. B. (2010). Cis-interactions between Notch and Delta generate mutually exclusive signalling states. *Nature* **465**, 86-90.
- Usui, K. and Kimura, K. (1992). Sensory mother cells are selected from among mitotically quiescent cluster of cells in the wing disc of *Drosophila*. *Development* **116**, 601-610.
- Usui, K. and Kimura, K.-i. (1993). Sequential emergence of the evenly spaced microchaetes on the notum of *Drosophila*. *Roux's Arch. Dev. Biol.* **203**, 151-158.
- Vidwans, S. J. and Su, T. T. (2001). Cycling through development in *Drosophila* and other metazoa. *Nat. Cell Biol.* **3**, E35-E39.
- Zitserman, D. and Roegiers, F. (2011). Live-cell imaging of sensory organ precursor cells in intact *Drosophila* pupae. *J. Vis. Exp.* **51**, e2706.

Supplemental Information



Movie S1, related to Figure 1. SOP pattern development. Notum genotype: shotgun:GFP, neuron GAL4, UASn GMCA. Anterior to the right. Scale bar, 50μm. Timelapse (upper left, hh:mm), 1 frame = 30 minutes.

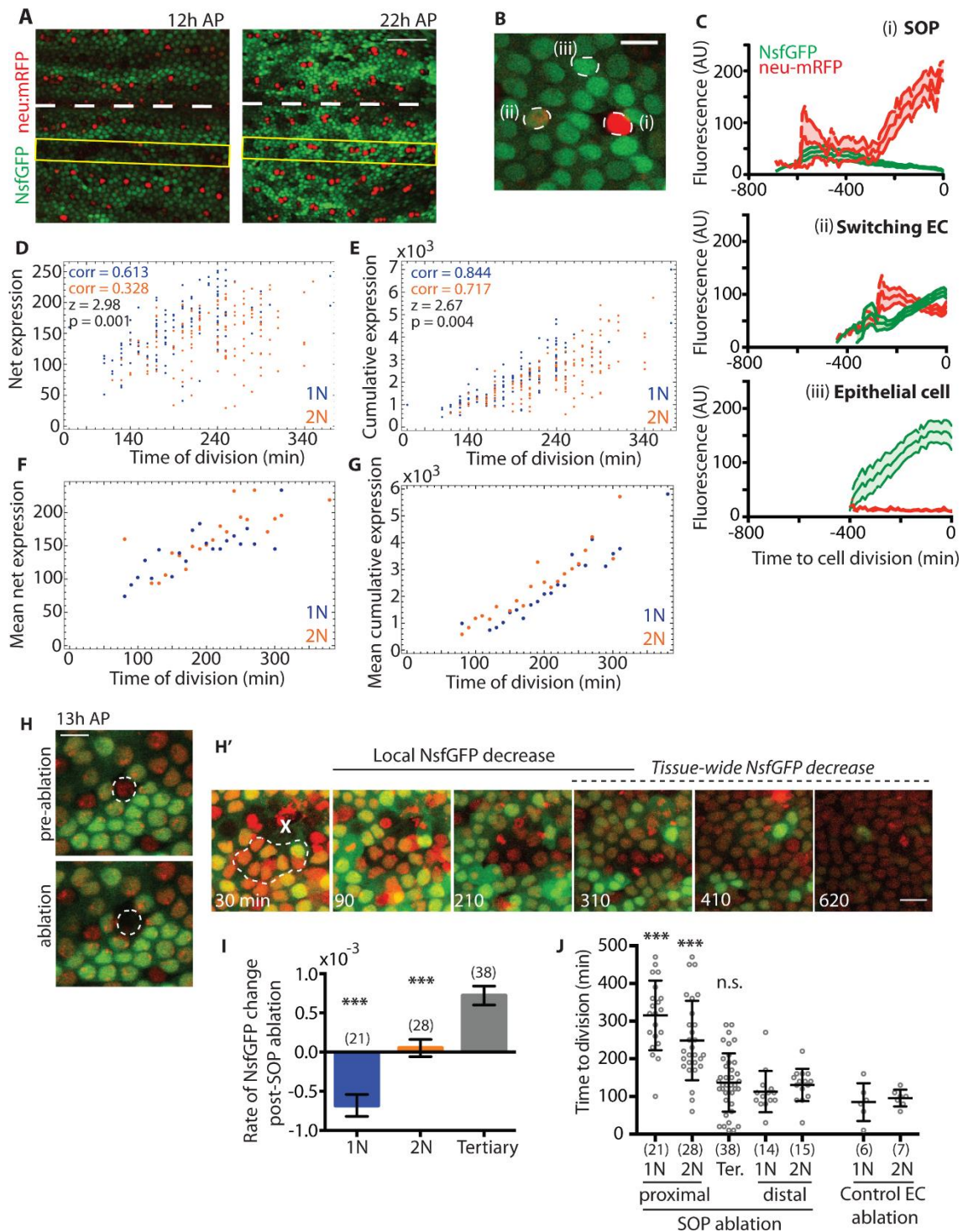


Figure S1, related to Figure 2. (A) Notum expressing NsfGFP (green) indicating Notch response and neu-mRFP (red) indicating pro-neural gene expression at 12 and 22h AP. Dashed line indicates midline. Yellow box highlights bristle row 2. Unless otherwise indicated, NsfGFP measurements were made for developing SOP neighbourhoods in row 2. Scale bar, 50µm. (B) NsfGFP and neu-mRFP expressing notum cells, indicating cells expressing (i) only pro-neural reporter, (ii) both reporters, or (iii) only Notch reporter. Scale bar, 10µm. (C, i-iii) Corresponding NsfGFP and neu-mRFP dynamics in (i) SOP cells (n = 7, N = 2), (ii) cells expressing both reporters (n = 35, N = 3), and (iii) epithelial cells (n = 6, N = 1). Mean ± SEM. (D, E) Plot of individual data points corresponding to net (D) or cumulative (E) NsfGFP expression. (F) Mean net NsfGFP levels at the time of division increases with time of division. (G) Mean cumulative NsfGFP expression increases with time of division. (D-G) n=266 cells, N=3 nota; corr = Pearson's correlation coefficient, z-value = Fisher r-to-z transformation, p-value = one-tailed test, 1N>2N. (H) Notum expressing NsfGFP (green) indicating Notch response and ubi-H2B-mRFP (red) indicating nuclei 13h AP. Pre-ablation and post-ablation panels, targeted SOP cell is outlined. In pre-ablation image, the indicated SOP is the only SOP in the panel. Scale bar, 10µm. (H') Example of post-ablation tissue (from region in H). White dashed line indicates cells that are primary and secondary neighbours to the ablated SOP cell (marked with X). Local NsfGFP decrease precedes tissue-wide NsfGFP decrease, suggesting that loss of SOP leads to acute loss of Notch response. Cell division occurs (*e.g.*, see panel at 310 min) and epithelium heals. (I) Rate of change of normalized NsfGFP fluorescence in ECs neighbouring an ablated SOP cell as in (H'). 1N, primary neighbour to ablated SOP; 2N, secondary neighbour to ablated SOP; tertiary, cells 2N+ to ablated SOP,

but $\leq 2N$ to an nearby, intact, SOP. Data generated from a total 5 ablations performed across 3 pupae, (n) = number of cells. Rate measured from onset of timelapse imaging, beginning 30 min after ablation, $\sim 13.5h$ APF. *** $p \leq 0.001$, One-way ANOVA, multiple comparisons, comparing to tertiary cells. Mean \pm S.D. shown. (J) Cell division is delayed following SOP ablation. 1N, proximal: primary neighbour to ablated SOP; 2N, proximal: secondary neighbour to ablated SOP; ter.: tertiary cells as defined in (I); 1N, distal: primary neighbours to an intact SOP in same notum as proximal cells, but $>100 \mu m$ away (as a developmental timing control); 2N, distal: secondary neighbors to an intact SOP in the same notum as proximal cells, but $>100 \mu m$ away; 1N, control EC ablation: primary neighbor to an ablated EC (SOPs intact, as a wounding control); 2N, control EC ablation: secondary neighbor to an ablated EC (SOPs intact). Two control EC ablations were performed in one pupae. (n) = number of cells. T = 0 at $\sim 13.5h$ AP. Mean \pm S.D. shown. *** $p \leq 0.001$, by One-way ANOVA, multiple comparisons, comparing to tertiary cells. N.s., by one-way ANOVA using control 1N groups.

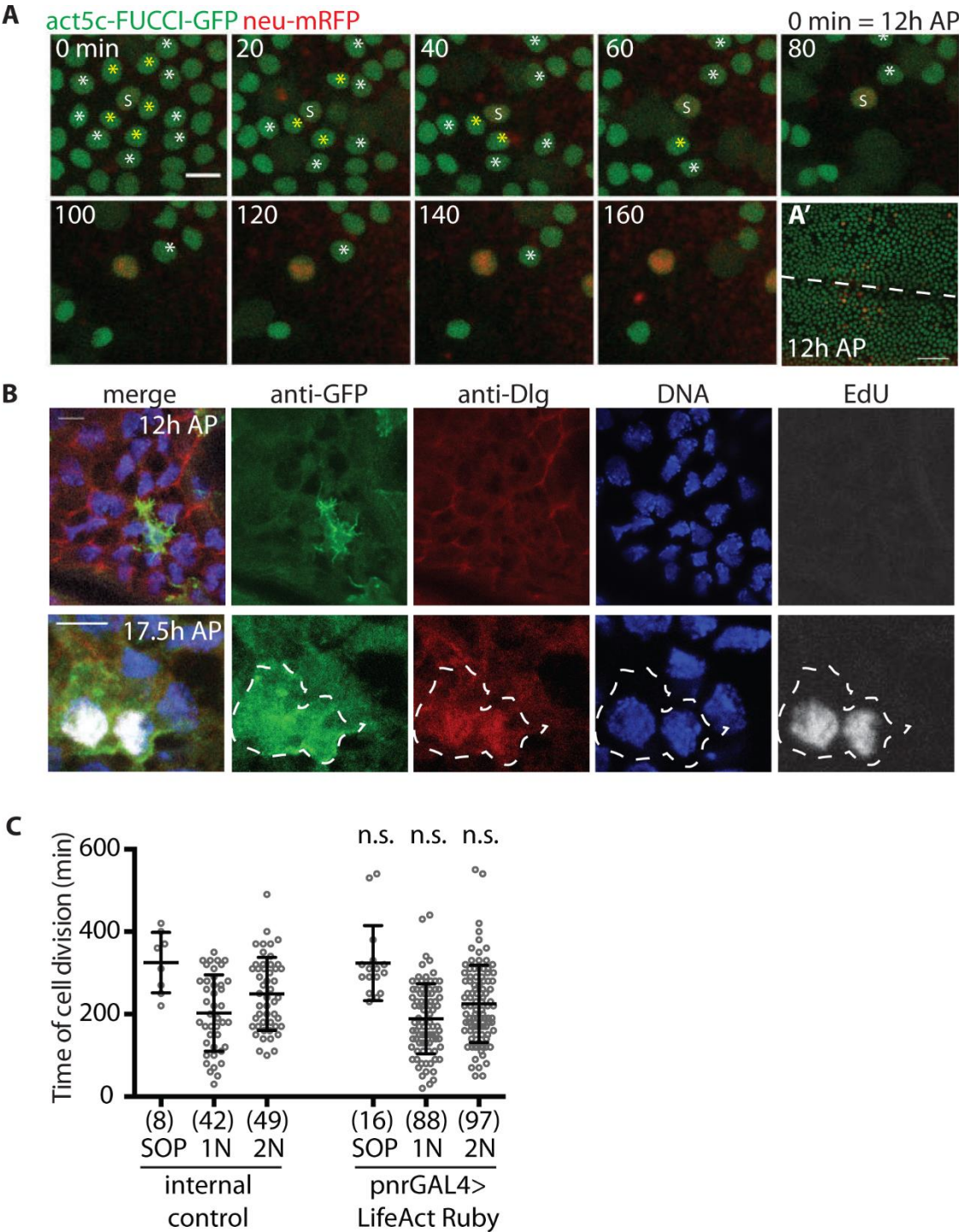


Figure S2, related to Figure 3. (A) act-FUCCI-GFP (green) and neu-mRFP (red). Loss of GFP signal indicates G2-exit. S, SOP cell; yellow asterisk, 1N; white asterisk, 2N. Scale bar, 10 μ m. (A') Zoomed out image of full FUCCI-GFP expressing nota; scale bar, 50 μ m, dashed line indicates midline. All cells are in G2. (B) 12h (upper panels) and 17.5h (lower panels) AP nota labeled with EdU to indicate absence of ECs in S-phase; cell cycle progression in SOP cell lineage serves as a control. Genotype: neu-GAL4, UAS-GMCA; thus anti-GFP panels visualize GMCA/F-actin in SOP or SOP daughter (pIIa/pIIb) cells. Dashed white line outlines pIIa/pIIb cell bodies. Scale bar, 5 μ m. (C) Cell division timing in shotgun^{GFP}, neu-GMCA; pnrGAL4 > UAS-LifeActRuby control pupae (N=2, n = as noted). N.s., not significant by unpaired t-test, compared by cell type (i.e., 1N inside vs 1N outside). Cells counted outside pnr domain as internal control to inside pnr domain UAS expressing cells.

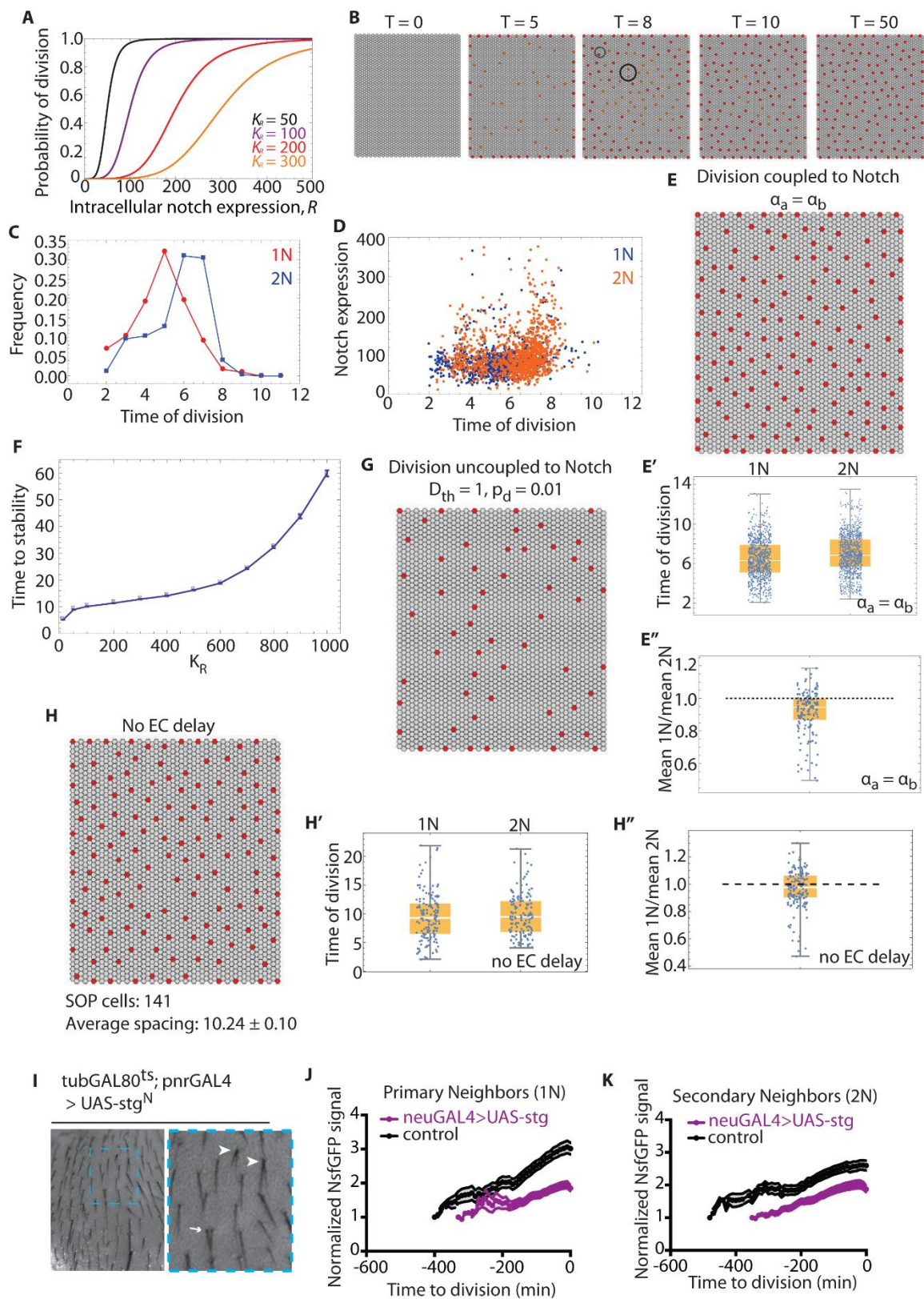


Figure S3, related to Figure 4. (A) Probability of division for given values of K_R and $q=5$. (B) Time course of 'wildtype' pattern, $R_{th} = 200$, $p_d = 0.5$. Red cells = high Delta; Orange cells = intermediate; Uncolored/gray = high Notch. Circles indicate local, transient pattern disruptions that are resolved. (C) Frequency of divisions for the wildtype model by time-step. (D) Level of Notch expression (AU) at division time for dividing cells in the wildtype model. (E) Model output when cell division is coupled to Notch but $\alpha_a = \alpha_b$. (E') Timing of 1N and 2N cell divisions when $\alpha_a = \alpha_b$. (E'') Local ratio of mean 1N and mean 2N time of divisions when $\alpha_a = \alpha_b$. (F) Time to stability for given values of R_{th} . Stability is defined as >2 AU of time without cell fate changes in the pattern. (G) Final time point for simulations where cell division is uncoupled from Notch signaling for D_{th} and p_d indicated. (H) Model output when cell division is coupled to Notch but independent of protrusion length, with $\alpha_a = 0$, $\alpha_b = 1.2$ (thus 1N and 2N ECs have equivalent incoming Notch signal; there is no delay between mean 1N and mean 2N division time) (H') Timing of 1N and 2N cell divisions and (H'') local ratio of mean 1N and mean 2N time of divisions for simulation as in (H). (I) Adult dorsal thorax microchaete patterns of the genotypes indicated. Anterior to the top of each panel. Arrowheads indicate split microchaete; arrow indicates 'twin' adjacent microchaete. (J) N^{sfGFP} signal dynamics in wild type primary or (K) secondary ECs neighbouring SOPs overexpressing *cdc25/string* (*stg*) under *neu-GAL4* (purple; $n=28$, $N=3$) or control SOPs (black; *neuGAL4*, *UAS-lifeActRuby*; $n=30$, $N=3$). Mean \pm SEM shown.

Supplemental Experimental Procedures

Fly strains. Drivers: tub-GAL80^{ts}/CyO; neuralized-GAL4, UAS-GMCA/TM6B

neu-GAL4, UAS-GMCA/TM6B

shotgun^{GFP}; neu-GAL4, UAS-GMCA/TM6B

shotgun^{GFP}, neu-GMCA/CyO-GFP; pnr-GAL4/TM6B

N^{sfGFP}/CyO-GFP; pnr-GAL4/TM6B

N^{sfGFP}/CyO-GFP; neu-GAL4/TM6B

Responders: UAS-wee1RNAi; UAS-myt1RNAi; UAS-stg RNAi; UAS-Su(H) RNAi;

UAS-lifeActRuby; UAS-string^N.

Other: N^{sfGFP}; act-FUCCI-GFP; neuralized-nls:mRFP

Immunofluorescence. Nota were fixed in 4% formaldehyde / 1x PBS (Sigma) and washed to permeabilize with 1x PBS with 0.01% Triton X-100 (1x PBST). Samples were blocked (50% blocking buffer: 3% FBS, 5% BSA in 1x PBS) for 1h at room temperature. Primary antibodies (anti-Discs-large, DSHB 4F3, Parnas et al., Neuron 2001; anti-GFP, AbCam, ab#13970) were added to 5% blocking buffer in 1x PBST to concentrations listed, and incubated overnight at 4°C. Samples were washed several times with 1x PBST, and incubated in secondary antibody in 1x PBST at room temperature for 2-4 h. Where needed, nota were further incubated for 20 min at room temperature with phalloidin (Acti-stain 555 phalloidin, Cytoskeleton PHDH1-A, 1:500) and DAPI (Molecular Probes D1306, 1:1000) or Hoechst33342 (provided with Clk-it EdU kit, ThermoFisher C10340, 1:2000). Final washes in 1x PBST were followed by overnight equilibration in mounting media (50% glycerol/1x PBS).

Mathematical Methods in Full

Protein dynamics

We used a mathematical model to simulate lateral inhibition by Delta-Notch signalling. The model is defined by a set of coupled differential equations (based on (S1)), which describe the dynamics of Notch (N_i), Delta (D_i) and a Reporter of Notch signalling (R_i) for individual cells:

$$\frac{dN_i}{dt} = \beta_N - \frac{N_i D_{trans}}{k_t} - \frac{N_i D_i}{k_c} - \gamma_N N_i \quad (1)$$

$$\frac{dD_i}{dt} = \beta_D \frac{1}{1 + R^m} - \frac{N_i D_{trans}}{k_t} - \frac{N_i D_i}{k_c} - \gamma_D D_i \quad (2)$$

$$\frac{dR_i}{dt} = \beta_R \frac{(N_i D_{trans})^s}{k_{RS} + (N_i D_{trans})^s} - \gamma_R R_i \quad (3)$$

The parameters β_N , β_D , β_R and γ_N , γ_D , γ_R are the production and degradation rates of Notch, Delta and the Reporter of Notch signalling respectively. The constants k_t and k_c determine the strength of Delta-Notch interactions in trans and in cis respectively, and k_{RS} is the dissociation constant for the intracellular signal. D_{trans} and N_{trans} indicate the incoming Delta and Notch signal and are determined by summing the signal from all contacting cells, scaled by a factor α_a and α_b for apical and basal contacts respectively. We normalized these values so that $\alpha_a = 1$ and $\alpha_b = 0.2$. These relative weights for apical and basal signalling are in agreement with previously measured values, although our model is relatively robust to changes in α_b (S2). A Gaussian noise term was applied to initiate protein concentrations and to the concentrations at each time step.

Protrusion dynamics

Basal protrusions were implemented as 2D circular areas, extending from the centre of each cell. Radii were drawn from a normal distribution with mean $F_{mean} = 5.6$ (2.3 times the cell diameter) and variance 0.3 (S2). A contact probability term was introduced to account for the angular directions of protrusions that were observed and hence the associated likelihood of two protrusions signalling to each other at different ranges. This was implemented in the model by assigning each cell a randomly selected ‘direction’ term, r , an integer between 1 and 100. For any two cells ($cell_1$ and $cell_2$) spaced a distance, d , such that their protrusions are of sufficient length to signal, a signal occurs if the condition is met such that:

$|vertr_{Cell_1} - r_{Cell_2}| < \frac{P}{d^2}$, where P was a constant variable. Hence the likelihood of a contact being made

reduced in proportion to the square of the distance between two cells. At each time step a random number generator was used to determine whether the protrusions of a particular cell (i.e. the length and directionality of the protrusion) would be updated. Thus, protrusion lifetimes were set according to a Poisson distribution.

Cell division

We model cell division in wild-type flies by assuming that *cdc25* activity is coupled to the expression of the intracellular Notch reporter, R . The cumulative expression of R at division scales linearly with the division time in control experiments, whereas the value of R itself appears to fluctuate within a confined window (Fig. 3). These data suggest that cells respond to the absolute, rather than cumulative, signal expression, and divide with a probability that is a function of their intracellular Notch expression. To model cell division in this manner, we define,

$$p_d = \frac{R^q}{K_R^q + R^q} \quad (4)$$

where p_d is the probability that a cell divides within a each time step in our simulations, K_R is the hill function dissociation constant and determined the range of values of R for which division is likely. We note that a similar set-up where *cdc25* was coupled to the cumulative expression of the Notch reporter gave similar results (not shown). Cells that have divided maintain their expression levels prior to division but no longer participate in lateral signalling so that they are excluded from the calculation of N_{trans} and D_{trans} for other cells. Also note that we set a threshold in the simulation time t_{th} below which cells cannot enter division. This is important in the model because the early dynamics of Delta-Notch are so that most cells go through transient phases where they express both proteins and we want to avoid division at that stage (S3).

Simulation Parameters

The same baseline parameters used for all simulations: $\beta_N = 100$, $\beta_D = 500$, $\beta_R = 300000$, $\gamma_N = \gamma_D = \gamma_R = 1$, $k_t = k_c = 1$, $k_{RS} = 10000000$, $m = 2$, $s = 2$, $q = 5$, $F_{mean} = 5.6$, $F_{se} = 0.3$, $F_{rate} = 10$, $error = 0.01$, $\alpha_a = 1$, $\alpha_b = 0.2$, $P = 1000$ and $t_{th} = 2$. Initial expression values were sampled from a Normal distribution $N(10^{-3}\beta_N, 10^{-4}\beta_N)$ and $N(10^{-3}\beta_D, 10^{-4}\beta_D)$ for Notch and Delta respectively. All R values were initially set to 0. The cell radius was set equal to 2. We varied the division rule (e.g. dependence on

Delta or intracellular Notch expression), in individual simulations as summarized in each figure legend.

The model was applied to a uniform hexagonally packed 2D array of 50x50 cells. Simulations were performed by numerically solving equations (1)-(3) using the Euler method. The Euler step was set to 0.005 and all simulations were run until stability was reached (defined as no changes in cell fate for 2a.u. of time), which was within $T=40$ a.u. in simulation time.

Supplemental References

[S1]. Sprinzak D, Lakhanpal A, LeBon L, Garcia-Ojalvo J, Elowitz MB. Mutual Inactivation of Notch Receptors and Ligands Facilitates Developmental Patterning. PLoS Comput Biol. 2011 7(6):e1002069.

[S2]. Cohen M, Georgiou M, Stevenson NL, Miodownik M, Baum B. Dynamic filopodia transmit intermittent Delta-Notch signaling to drive pattern refinement during lateral inhibition. Dev Cell. 2010 Jul 20 19(1):78-89.

[S3]. Collier JR, Monk N a, Maini PK, Lewis JH. Pattern formation by lateral inhibition with feedback: a mathematical model of delta-Notch intercellular signalling. J Theor Biol. 1996 183(4):429-46.